HIGH DISCHARGE RATE CHARACTERISTICS OF NICKEL-CADMIUM BATTERIES
FOR PULSE LOAD FILTERING[1]

Gregory M. Gearing and Michael B. Cimino
Air Force Institute of Technology

David H. Fritts and John F. Leonard
Air Force Wright Aeronautical Laboratories

Andrew J. Terzuoli, Jr.
Air Force Institute of Technology

ABSTRACT

This investigation consisted of several tests of specially fabricated nickel-cadmium batteries having circular disk type electrodes. These batteries were evaluated as filter elements between a constant current power supply and a five hertz pulsed load demanding approximately twice the power supply current during the load on portion of the cycle. Short tests lasting 10^4 cycles were conducted at up to a 21 C rate and an equivalent energy density of over 40 Joules per pound. In addition, two batteries were subjected to 10^7 charge/discharge cycles, one at a 6.5 C rate and the other at a 13 C rate. Assuming an electrode to battery weight ratio of 0.5, these tests represent an energy density of about 7 and 14 Joules per pound respectively. Energy density, efficiency, capacitance, average voltage, and available capacity were tracked during these tests. After 10^7 cycles, capacity degradation was negligible for one battery and about 20% for the other. Cadmium electrode failure may be the factor limiting lifetime at extremely low depth of discharge cycling. The output was examined and a simple equivalent circuit was proposed.

INTRODUCTION

This investigation consisted of several tests of specially fabricated nickel-cadmium batteries having circular disk type electrodes. These tests addressed three areas. First, would the circular electrodes increase the maximum energy density when compared to standard aircraft batteries. Secondly, what energy density could be maintained and achieve a lifetime of 10^9 cycles at 5 hertz. And finally, how does the battery influence the voltage and current waveforms to the load.

[1] The material reported herein is based on research conducted at and supported by the Air Force Wright Aeronautical Laboratories, Aero Propulsion Laboratory, Wright-Patterson AFB, Ohio.

A bi-polar geometry was considered optimum because of its lower internal resistance and inductance, enabling it to receive and deliver pulses of high current [1]. The reduced internal losses lead to greater efficiency and therefore the potential for a higher energy density. This reduction is achieved in part, by straightening and shortening the current path within the battery.

PSEUDO BI-POLAR BATTERY

Although the construction of bi-polar electrodes has been accomplished at a number of facilities, the fabrication of a bi-polar battery has been complicated by the lack of a reliable edge seal to prevent electrolyte shorting between cells. In order to take advantage of the bi-polar geometry without inheriting the edge seal problems, a pseudo bi-polar nickel-cadmium battery was designed. It resembles a monoblock type construction and consists of a stack of single cell button style batteries in which adjoining cells share a common wall and intercell connector. Figure 1 shows an exploded view of the battery design. To obtain some understanding of the effects of this design on internal losses and to be compatible with available test equipment, several four cell nickel-cadmium pseudo bi-polar batteries were constructed.

In order to further reduce internal losses, a circular electrode with a large central current tab to uniformly collect the current was selected. The electrode was a 3.3 inch diameter disc with the active material impregnated in an annular shape around the center 1.25 inch diameter current tab. Current flow within the electrode is radial and the maximum current path length from the tab to the edge of the electrode is approximately 1 inch. This is in contrast to typical nickel-cadmium aircraft batteries which have rectangular electrodes with a current tab in one corner.

Figure 2 illustrates the differences between the test battery's electrode and that of a typical rectangular battery's electrode. The cross hatched areas are the regions of highest current density. For rectangular electrodes, this area lies between the positive and negative current tabs, and has been identified as a stress point associated with sealed battery failures. An increased current density accelerates the cadmium to cadmium hydroxide to cadmium formations that occur during battery charge and discharge. With pellon or nylon as the separator material, as used in sealed nickel-cadmium cells, cadmium crystals become lodged in the separator eventually shorting out the cell [2]. Although the circular tab does not eliminate this problem, it is a step towards a bi-polar design where the peak current density is spread more uniformly over a larger area of the electrode, thereby reducing the stress and attendant failure mechanisms.

The cells are electrically connected by a 1.125 inch diameter, 0.210 inch thick nickel slug mounted in the plexiglas wall. The large cross section and relatively short intercell path length result in both a smaller internal resistance and inductance through the battery. The nickel to plexiglas seal was established by an O-ring around the nickel slug.

The positive nickel electrodes were obtained from Eagle Picher Industries. The plaque material was a standard 0.030 inch thick nickel sinter (dry sinter process) with a porosity of approximately 80%. They were electrochemically impregnated with 1.7 grams of active $NiO(OH)$ per cubic centimeter of void. The result was an electrode with approximately a 1.4 ampere hour theoretical capacity (C). In addition, to improve the electrode/nickel slug weld, Battery 7 was constructed with nickel electrodes fabricated at AFWAL/APL using an aqueous process [3], to approximately the same 1.4 ampere hour theoretical capacity.

The negative cadmium electrodes were fabricated at AFWAL/APL using a process developed and patented by Fritts, et. al. [4]. This process used the same base plaque, 0.030 inch thick 80% porosity nickel sinter. The electrodes were loaded with 6 to 8 grams of active cadmium each for a theoretical capacity of 2.5 to 3.1 ampere hours. This combination insured that the battery cells were nickel limited.

The cells were assembled by first welding the electrodes to the nickel slug/plexiglas wall combination. Then these units were stacked and glued one by one in a plexiglas tube. A relief vent (about 8 psi) was installed in each cell. Finally a reference electrode, a 1 millimeter diameter cadmium wire, was inserted into each cell. Leads were soldered on the outside of the end cells and a plexiglas stand was attached.

To fill the cells, the vents were removed and the battery was set upside down in a beaker of electrolyte (32% by weight KOH). A vacuum of 28 inches of mercury was pulled on the entire assembly. When the vacuum was released electrolyte was drawn into the cells. The procedure was repeated several times to insure electrode saturation.

FINDING A SEAL

One of the major problems with the construction and use of bi-polar batteries is obtaining a satisfactory intercell seal, thus keeping the electrolyte from shorting out adjoining cells. The first step in the fabrication of the test battery was to evaluate a neoprene O-ring placed around a nickel slug. This assembly was then inserted in the bottom of the test container as shown in Figure 3. The bottom of this container simulated an intercell wall. There was no noticeable electrolyte leakage in 30 days, with electrolyte under approximately 8 psi of pressure. This success, elimination of electrolyte leakage between cells, overcame one of the major stumbling blocks in bi-polar nickel-cadmium battery construction.

ELECTRODE TO CURRENT TAB WELDING

During the gluing of Battery 2, one cadmium electrode to nickel slug weld was broken. Rewelding was not possible, so construction was completed by placing the electrode in its proper place and relying on the pressure of the next layer to hold it there.

On batteries 4 through 7, the smooth side of a perforated nickel foil, typical nickel-cadmium current tab material, was welded to both sides of the nickel slug before the electrodes were attached. The rough side of the tab was driven into the electrode's center area tab by the spot welder. The resulting weld connected the nickel wire within the electrode to the nickel tab material. This weld proved to be stronger. However, one nickel slug to foil weld was broken (Battery 3) during assembly.

Temperature readings of the end terminals and case of Battery 4 during the extended cycle test indicated that the nickel terminal was hotter than the case or cadmium terminal. This was attributed to higher current densities due to the few welds remaining intact. To improve this weld, nickel electrodes with unimpregnated centers were produced for Battery 7.

ELECTRODE COMPARISON

Prior to final construction, the electrodes for each battery were weighed. The weight of each assembled battery, including electrolyte, was recorded. Separate weights were taken, since the overall battery container was not optimized for weight, but rather for ease of laboratory construction. As a comparison, the electrode weight of the batteries used by Bishop and Stumpff[2] was 6.40 pounds while their total battery weighed 11.71 pounds. Therefore, the electrode accounted for 54.65% of the total weight. This ratio was used to determine the weight used in energy density calculations. It is based on the assumption that with some technological improvements, the test battery's design would result in a similar electrode to battery weight ratio.

Another important factor in battery design is the electrode surface current density. In normal parallel plate construction, each side of an electrode acts as a separate electrode, so that one half of the current flows from the center screen through each side of the electrode. Bi-polar electrodes have only a single sided electrode, since the second side is the intercell foil connector. However, rather than metal foil separating the cells, as in a true bi-polar battery, this pseudo bi-polar nickel-cadmium battery used a nickel slug and plexiglas intercell wall with "double sided" electrodes.

For Bishop and Stumpff, the current density through the electrode frontal surface area, with a total current of 100 amperes, was 0.0458 amperes/cm^2. The test electrodes, although fabricated in a double sided configuration, were used as single sided electrodes since the time of charge and discharge, 100 milliseconds, did not allow any significant current flow from the back sides of the electrodes. As a result, the current density for the test batteries, based on a single sided current flow, was 0.1365 amperes/cm^2, with a charging/discharging current of 6.36 amperes. This results in possi-

[2] Unpublished AFWAL/APL test report regarding the testing of 5 series connected 22 ah ni-cd batteries at a charge/discharge current of 100 amps for 10^7 cycles at 5 hertz in 1983.

bly greater polarization at the electrode/electrolyte interface of the test batteries.

TEST SET UP

Figure 4 shows the equipment and circuit used for these tests. Two separate circuits were set up. The first had a 0-15 ampere load and the second had a 0-60 ampere load. A 0-50 amp, constant current, constant voltage power supply, was connected in parallel, and on opposite sides of the battery, with either a 0-15 ampere solid state load, or a 0-60 ampere solid state load. A 5 hertz square wave generator switched the load, simulating a 50% duty cycle current pulse load. A blocking diode on the output of each power supply prevented an inadvertent battery discharge back through the power supply. Current shunts were inserted to measure actual power supply current (I_S), load current (I_L), and battery current (I_B). Note that for battery charging I_B is negative and for discharging I_B is positive. Figure 5 shows typical voltage and current waveforms from this test circuit.

CONDITIONING THE BATTERY

Prior to testing the batteries, several charge/discharge cycles were completed to condition the batteries, stabilize their operation, and measure the initial capacity. The theoretical C rate of these pseudo bi-polar nickel-cadmium batteries was 1.4 ampere-hours. The charging rate was 0.75 amperes for the first two cycles and 1.5 amperes thereafter, until the total voltage reached 6.2 volts (1.55 volts/cell).

The battery was then discharged at a 1 ampere rate down to a total voltage of 4 volts. This cycling continued until the capacity was stable for two successive cycles. The measured capacity of each battery, after the initial conditioning cycles and after any additional testing, is shown in Table 1.

Since this experiment used a novel battery design, which did not have any demonstrated cycle life, the first series of tests were run under the same conditions (room temperature, 5 hertz cycle rate, 0.013% depth of discharge (DOD)) as Bishop and Stumpff's test. This provided a direct comparison of battery types.

ENERGY DENSITY

The first objective was to increase the energy density of the battery when used as a capacitive filter. Energy density is a function of the current through the battery (the voltage is nearly constant) and the weight of the battery. A five hertz test was run at various charge and discharge currents starting at five amperes and increasing in five ampere steps. Each current level was maintained for 10,000 cycles with data collection occurring after approximately 5000 cycles.

Battery 4 was tested up to 25 amperes or 18 times the C rate. By incorporating a larger load, Battery 7 was tested to 35 amperes, or 21 C. At this point, the exterior case reached 60°C and further increases were not attempted. The 60°C cutoff was an arbitrary level picked to insure internal temperatures would remain well below the boiling point of the electrolyte, approximately 100°C.

The resulting battery voltage and current plots were utilized to evaluate the average capacitance during discharge, the energy density, and efficiency of the battery.

CALCULATIONS

To calculate the energy into and out of the battery and average capacitance during discharge, the battery voltage was assumed to be a step increase/decrease followed by a linear ramp. The average ramp voltage was used as a constant value for the entire charge or discharge. The initial step change was due primarily to the instantaneous series resistance of the battery. The remaining ramp change was primarily a function of the double layer capacitances and faradaic discharge. Since the solid state loads and power supplies are not ideal devices, the battery was not reacting to a perfect step increase or decrease in current during the first few milliseconds of any cycle. Therefore, the calculations started after the load and power supply currents had stabilized, i.e., approximately 1 millisecond after the start of the load switching.

Figure 5 shows a typical waveforms from the test circuit. The voltage rate of change varied from about 9 volts/second during the first 20 milliseconds to 3 volts/second for the remaining 80 milliseconds. From Figure 5, the average voltage, using a straight line approximation, is 4.90 volts, while the integral of the voltage divided by the time gives an average of 4.86 volts. This approximation results in less than a 1 percent error.

MAXIMUM ENERGY DENSITY TESTING

Figures 6 through 8 depict the average capacitance, energy density, and efficiency as functions of DOD. At the higher current levels examined with Battery 7, it was observed that as battery voltage varied, so did the other parameters, particularly average capacitance. For example, at 30 amperes discharge current the end discharge voltage dropped below 4 volts. By increasing the average battery voltage from 5.1 to 5.3 volts, this low point was raised to approximately 4.25 volts, roughly the value recorded during the 25 ampere discharge test. This point coincides with the abrupt reversal of the average capacitance and efficiency in Figures 6 and 8. At the highest current, the test battery's equivalent energy density was over 40 joules per pound. In addition, it appears that battery discharge voltage has a significant effect on the voltage regulation, or effective average capacitance, and efficiency.

CYCLE LIFE

In order to project a possible cycle lifetime for the new design, two batteries were run for 10^7 cycles. Since this is only a small fraction of the proposed lifetime and no catastrophic failures occurred, no conclusive data was obtained. Figures 9 through 13 show average battery voltage, energy density, average capacitance, efficiency, and capacity versus cycles completed at DOD's of 0.013% and 0.025%. These DOD's, which reflect the depth of capacity discharged each cycle, not necessarily the actual state of charge, were based on the theoretical battery capacity, not the rated capacity.

The relatively low measured capacity, when compared to the theoretical capacity, may be due to incomplete conditioning of the batteries prior to testing. However, the main purpose was to demonstrate energy densities above 10 Joules/pound, document performance of the batteries over 10^7 cycles, and analyze the battery influence on voltage and current when used as a filter. Incomplete conditioning did not noticeably impede any of these objectives.

Although not a failure, Battery 3 had a varying internal resistance during the 10^7 cycle test. It was found that by increasing pressure on the end of the battery, the internal resistance would drop. After completing the testing, the battery was taken apart. In addition to a broken weld during construction, several other welds were very easy to break during dissection. The varying internal resistance is attributed to these poor welds.

Figure 13 shows the relative capacity of the test batteries before and after cycling. Battery 3 was reconditioned around 4.8 million cycles and therefore has three data points. As a comparison, the relative capacity measured by Bishop and Stumpff, from their test of 5 series connected 22 ampere/hour nickel-cadmium aircraft type cells is also included in Figure 13.

After completing the 10^7 cycle test, samples of both nickel and cadmium electrodes were examined and compared with uncycled electrodes. Photographs of these electrodes are shown in Figures 14 through 18. There was no apparent change in the nickel electrode. The cadmium electrode, however, showed a significant change. After cycling there were no large cadmium crystals left, only small ones, about 500 times smaller than those crystals found in an uncycled electrode. It is possible that the cadmium electrode may be the lifetime failure mechanism, as is typical of nickel-cadmium batteries in "normal" operations. Since most nickel-cadmium batteries are designed to be nickel electrode limited, this decrease would not show up until the cadmium capacity dropped below that of the nickel electrode. Post cycling capacity testing revealed that this was, in fact, the case for Battery 3.

Figure 13 shows the measured battery capacity versus number of cycles completed at a 5 hertz rate. Assuming that any decrease in measured capacity is attributable to a cadmium loss, the abrupt change in Battery 3's capacity could be attributed to the gradual failure of the cadmium electrode, finally dropping below that of the nickel electrode. Bishop and Stumpff's batteries

also show a fairly rapid decrease in measured capacity after about 5 million cycles, which may have also been a result of cadmium electrode deterioration.

Even with this increased rate of capacity loss, the test batteries appear to have lifetimes of 10^9 cycles or more. The dashed line in Figure 13 runs through the RMS values obtained from Batteries 3 and 4 at 5×10^6 and 10^7 cycles. It projects approximately a 50% remaining capacity at 10^9 cycles. Projecting this line back towards 1 cycle, results in a value of approximately 250% of initial battery capacity. This is roughly equivalent to about 80% of the initial theoretical cadmium capacity. However, there are still too few data points to accurately predict the lifetime of batteries when used as filters.

There were no identifiable trends or failures in energy density, average capacitance, or efficiency during the 10^7 cycles. Figures 10 through 12 only show the trends of these values through 10^7 cycles. Unless a catastrophic failure occurs, such as a complete short or open circuit, end of life performance criteria, such as effective average capacitance or efficiency, will have to be established before further testing can project an actual lifetime for these batteries when used as filter elements.

EQUIVALENT CIRCUIT

The third area of interest was to determine what effect a battery would have in a circuit when used as a filter element. During the energy density and 10^7 cycle testing, the power supply current was not constant. It appeared that the power supply output capacitors were charging and discharging faster than the battery during the first millisecond after the load switched on or off. To eliminate as many variables as possible, the battery was charged and then connected directly to the load without a power supply. The resulting voltage and current waveforms, together with those obtained during earlier testing, were used to form the basis for the proposed equivalent circuit below.

Each electrode had a volume of approximately 3.55 cm^3. Using a nickel Brunauer, Emmett, and Teller (BET) surface area to volume ratio of 70 m^2/cm^3, 2000 $\mu F/cm^2$ nickel capacitance to BET area, a cadmium BET surface area to volume ratio of 6 m^2/cm^3, and 50 $\mu F/cm^2$ cadmium capacitance to BET area ratio [5,6], the theoretical double layer capacitances were calculated. The nickel double layer capacitance is approximately 5000 farads and the cadmium double layer capacitance is approximately 11 farads.

The change in voltage due to the faradaic discharge for the batteries at a 5 C rate for 0.1 seconds at a 50% state of charge is approximately 0.14 millivolts. This term was neglected since it was over 1000 times less than observed voltage changes. Most of the discharge then, would appear to be across the cadmium capacitances since they are over 100 times smaller than the nickel capacitances.

296

Combining 4 cells in series gives the proposed battery equivalent circuit shown in Figure 19. E_1 is the combination of the nickel electrode voltage, resistance, and double layer capacitance. R_3 is the series ohmic resistance through the electrolyte, electrodes, and current tabs. C_2, E_2, and R_2 represent the cadmium electrode double layer capacitance, voltage across the electrode/electrolyte interface, and electrode/electrolyte ionic activation resistance respectively.

The equivalent circuit of Figure 19 results in an equation for the total battery voltage of:

$$V(t) = E_o - 4iR_3 - 4iR_2[1 - \exp(-t/R_2C_2)] \qquad (1)$$

where

$V(t)$ = Total Battery Discharge Voltage over Time
E_o = Initial Voltage before Discharge
i = Total Discharge Current
t = Time of Discharge
R_2 = Cadmium/KOH Ionic Activation Resistance
R_3 = Series Electrolytic Ohmic Resistance
C_2 = Cadmium Double Layer Capacitance

From battery voltage curves, $4R_3$ was between 20 and 57 milliohms for Battery 3 and 28 to 38 milliohms for Battery 4. Taking the initial rate of change of voltage from the discharge voltage waveform obtained during the early part of the 10^7 cycle test and using the equation $i=C(dv/dt)$, $(1/4)C_2$ was approximately 0.3 farads. After the 10^7 cycle test, it was not possible to determine C_2, although it appeared to have decreased significantly.

After determining $4R_3$ from the instantaneous change of voltage at both the beginning and end of the discharge, $4iR_2$ was assumed to be the remaining voltage drop occurring during the discharge. Solving for $4R_2$ gave a value of approximately 54 milliohms for both Battery 3 and 4.

Using these values and equation (1), $V(t)$ was plotted against the actual voltage waveforms for Batteries 3 and 4 as shown in Figures 20 and 21. Figure 22 shows the calculated $V(t)$ and actual voltage of Batteries 3 and 4 connected in series. The equation for $V(t)$ then became:

$$V(t) = E_o - 8iR_3 - 8iR_2[1 - \exp(-t/R_2C_2)] \qquad (2)$$

The same values obtained before for C_2, R_2, and R_3 were used as well as the actually measured current and initial voltage. This verifies that the equivalent circuit in Figure 19 appears to be reasonable approximation for these batteries when used as a capacitive filter.

When running the maximum energy density test with Battery 7, the voltage and current waveforms were recorded to evaluate the equivalent circuit of Figure 19. However, the values obtained for R_2, R_3, and C_2 varied as the discharge current and battery voltage varied. $4R_2$ ranged from 12 to 40 milliohms, $4R_3$ ranged from 18 to 35 milliohms, and $(1/4)C_2$ varied from 0.14 to 1.66 farads. It also appeared that at discharge currents above 10 C that the nickel double layer capacitance could no longer be ignored. Furhter analysis of this, which would appear to involve a more complet equivalent circuit, was beyond the scope of this paper.

As the number of cycles on the batteries increased, the voltage curve became initially steeper and then flatter, suggesting that the cadmium double layer capacitance may be decreasing. This may be attributed to the breakdown of the cadmium crystals causing the active electrode surface area to decrease.

If this is the case, a more uniform voltage output, excluding the first 5 milliseconds or so of each pulse, may be obtained by conditioning the battery, causing the cadmium capacity and capacitance to decrease. The nickel double layer and faradaic capacitances would then dominate (after the first 10 milliseconds) giving a much higher effective capacitance over the discharge cycle for the battery. However, this will leave a larger rate of change of voltage at the beginning of each discharge period, possibly allow the battery to become cadmium electrode capacity limited more quickly, and possibly reduce the battery lifetime.

DISCHARGE WITHOUT POWER SUPPLIES

To minimize test circuit induced stray inductance and capacitance on the waveforms of the battery while cycling, the power supply was disconnected. The battery was then connected directly across the load with a minimum of test circuit wiring. The resulting waveforms showed that the test circuit induced inductance was minimal, but the power supply capacitors charged and discharged during the first millisecond of each load change. This caused the power supply current to fluctuate so that the battery was not required to supply an instantaneous change in current. After the first millisecond the power supply and load currents were essentially constant. Therefore, analysis was started after one millisecond and is an accurate indication of battery operation, even with the power supply connected to the battery.

CONCLUSION AND RECOMMENDATIONS

In summary, a maximum equivalent energy density of over 40 joules per pound was demonstrated by the specially constructed test nickel-cadmium batteries. Ten million cycles at a 5 hertz rate with a useful equivalent energy density of 14 joules per pound were completed. Capacity degradation was negligible for one battery and only a 20% decrease for the other. Cadmium electrode failure may be the factor limiting lifetime. An equivalent circuit was derived, but further testing will be required to completely evaluate the results. Internal resistances and double layer capacitances

varied with changes in either battery voltage or current, suggesting that a more complex equivalent circuit may be required.

Batteries appear to be a competitive alternate to capacitors. Further research and testing needs to be accomplished in several areas. First, begin a long term life cycle test, 10^8 cycles or more, to obtain more conclusive data on the battery's long term capability to function as a filter element. Second, construct a bi-polar battery, if necessary achieving an intercell seal at the expense of weight, to determine if a bi-polar design would significantly improve the electrical characteristics desired. If successful, this would support large scale efforts to achieve a true lightweight bi-polar design. Third, begin more detailed experimentation to investigate the relationships between SOC, DOD, energy density, efficiency, output response, average voltage, and average effective capacitance to identify optimum operating conditions and devise a control system to maintain those conditions. Fourth, in view of the dramatic change in the cadmium structure, further analysis is needed to identify exactly what changes are taking place in the electrode, and how these changes will effect the long term performance of the battery when used as a filter element.

REFERENCES

1. Bauer, P.: Batteries for Space Power Systems. Washington D.C.: NASA, 1968. (NASA SP172).

2. Fritts, D.H. and Dueber, R.E.: Inhibiting Cadmium Migration in Nickel-Cadmium Cells by the Addition of Boron Compounds. The Electrochemical Society Fall Meeting, Extended Abstracts-Battery Division 100, New Orleans, Louisiana, 7-12 October 1984.

3. Pickett, D.F.: U.S. Patent 3,827,911, 1974.

4. Fritts, D.H.; et. al.: Methods of Fabricating Cadmium Electrodes, U.S. Patent 4,242,179, December 30, 1980.

5. Amile, R.F.; Ockerman, J.B.; and Ruetshci, P.: Absorption of Hydrogen and Oxygen on Electrode Surfaces. Journal of the Electrochemical Society, 108: 377, 1961.

6. Milner, P.C.; and Thomas, U.B.: The Nickel-Cadmium Cell. Advances in Electrochemistry and Electrochemical Engineering, Vol 5. 1-86. Edited by C.W. Tobias. New York: Interscience Publishers, 1967.

Table 1. MEASURED BATTERY CAPACITY (ampere hours)

BATTERY NUMBER	INITIAL CAPACITY	FINAL CAPACITY
1	0.1	0.0 (INTERCELL SHORT)
2	0.8	0.0 (INTERCELL SHORT)
3	1.0	0.8
4	0.95	0.93
5	0.63	NOT TESTED
6	NOT USED (INTERCELL SHORT)	
7	0.75	1.01
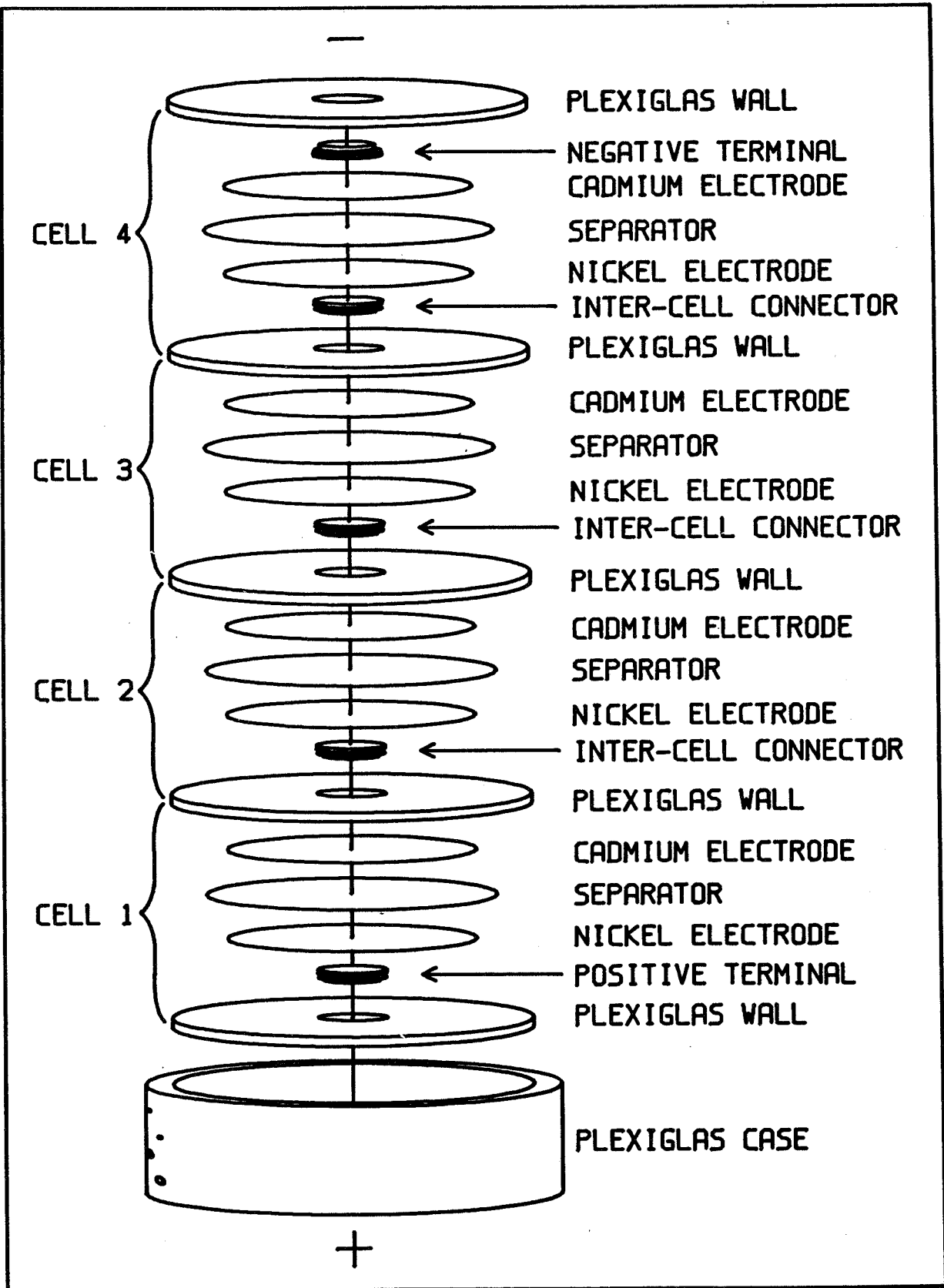
Figure 1. Expanded View of the Test Battery
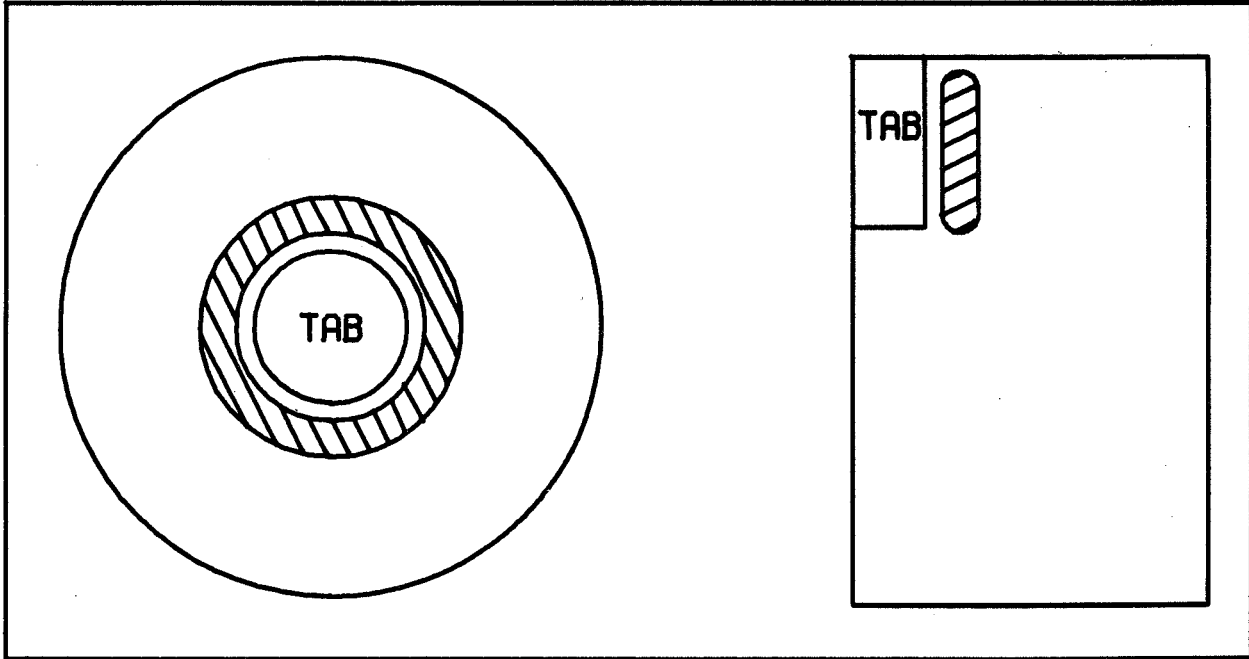
Figure 2. Circular Versus Rectangular Electrodes
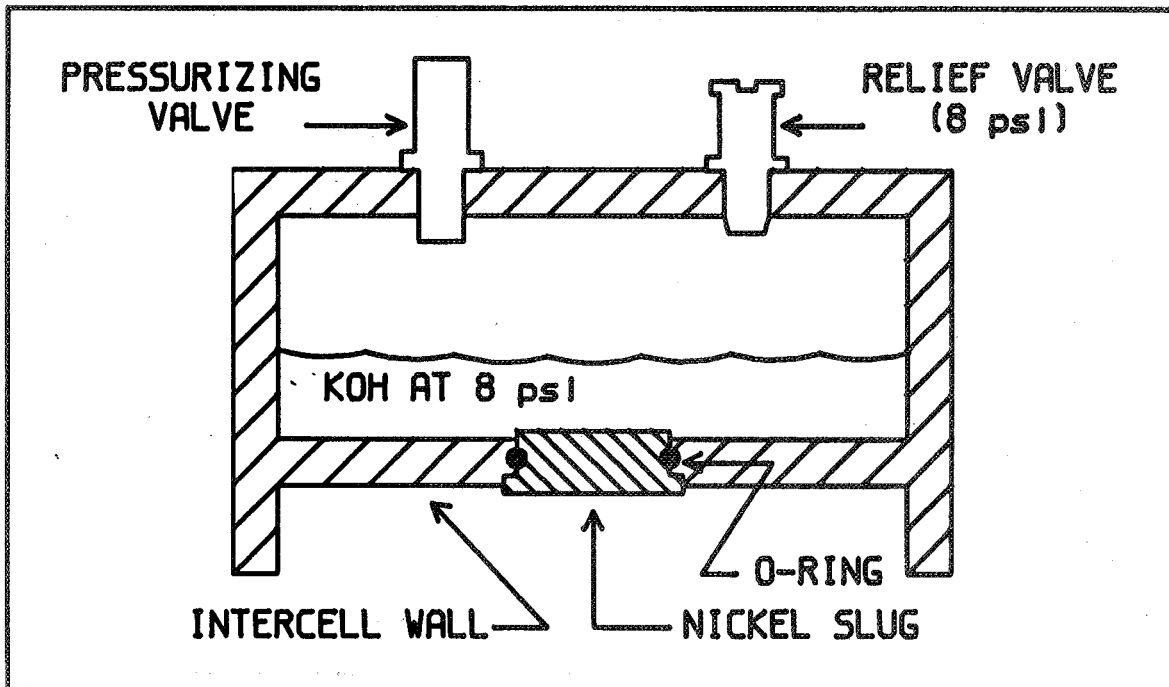
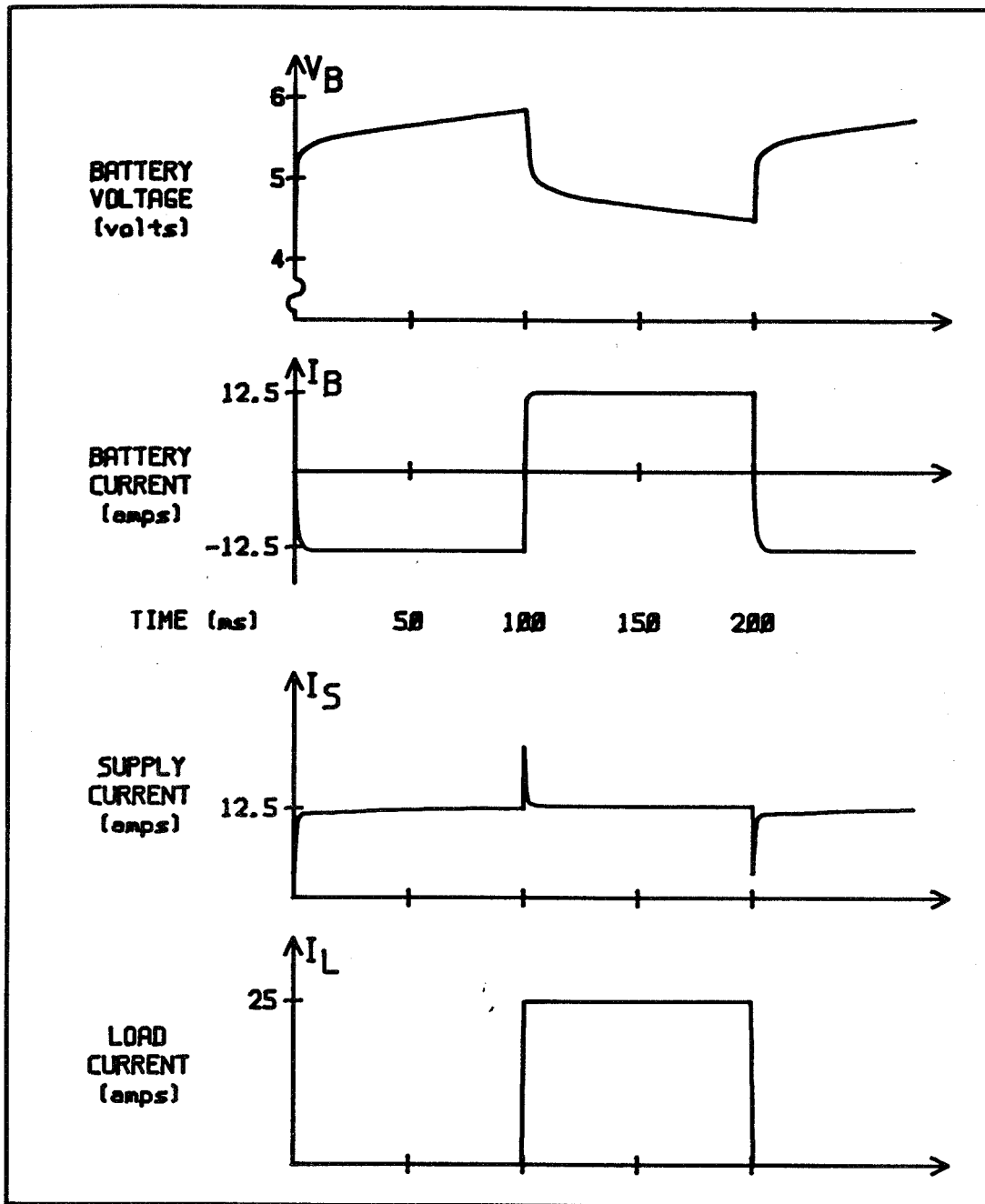Figure 3. Cutaway of O-Ring Seal Test Container
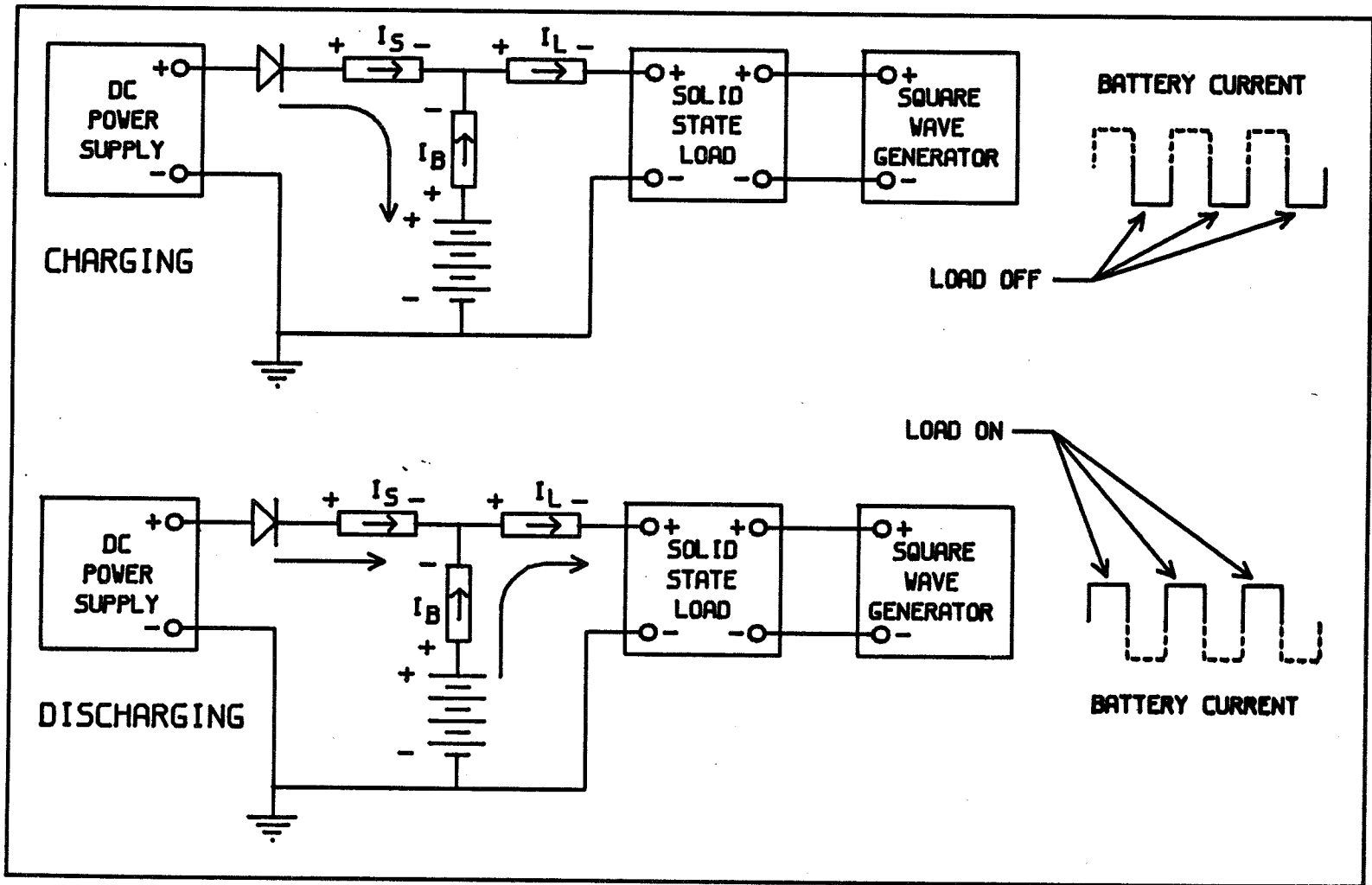
Figure 4. Test Circuit

Figure 5. Typical Waveforms

305
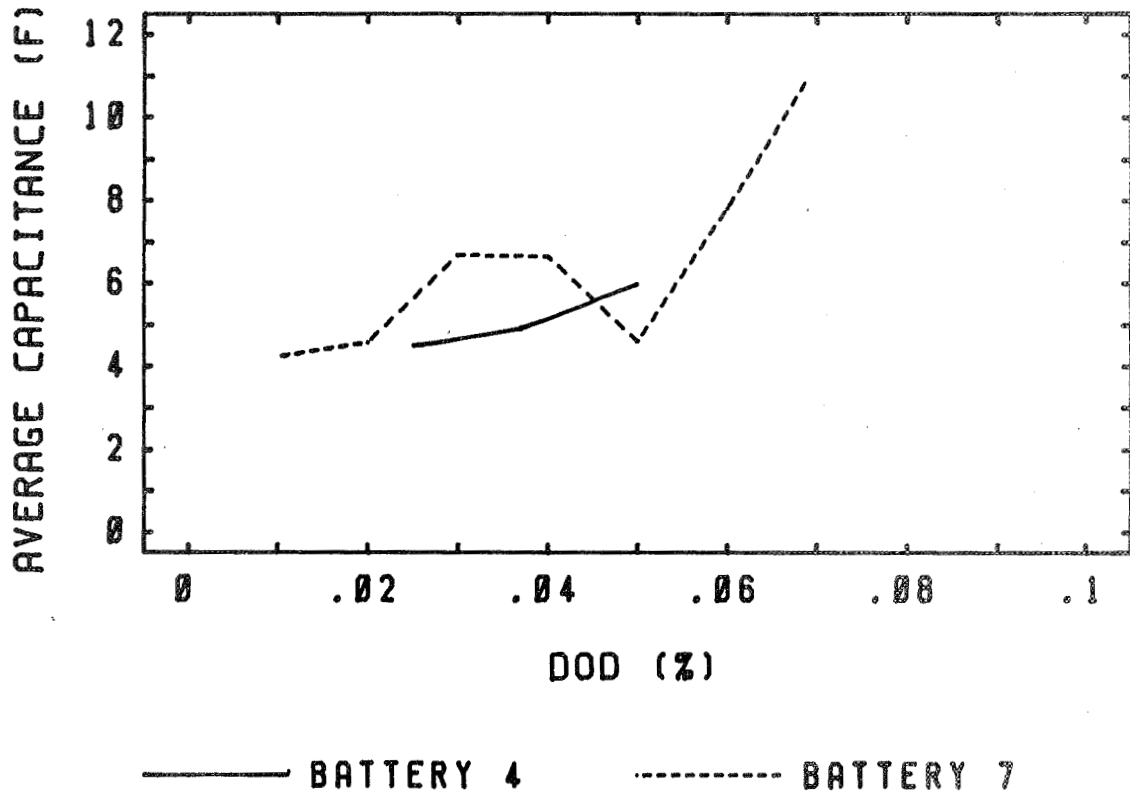
Figure 6. Average Capacitance Versus DOD
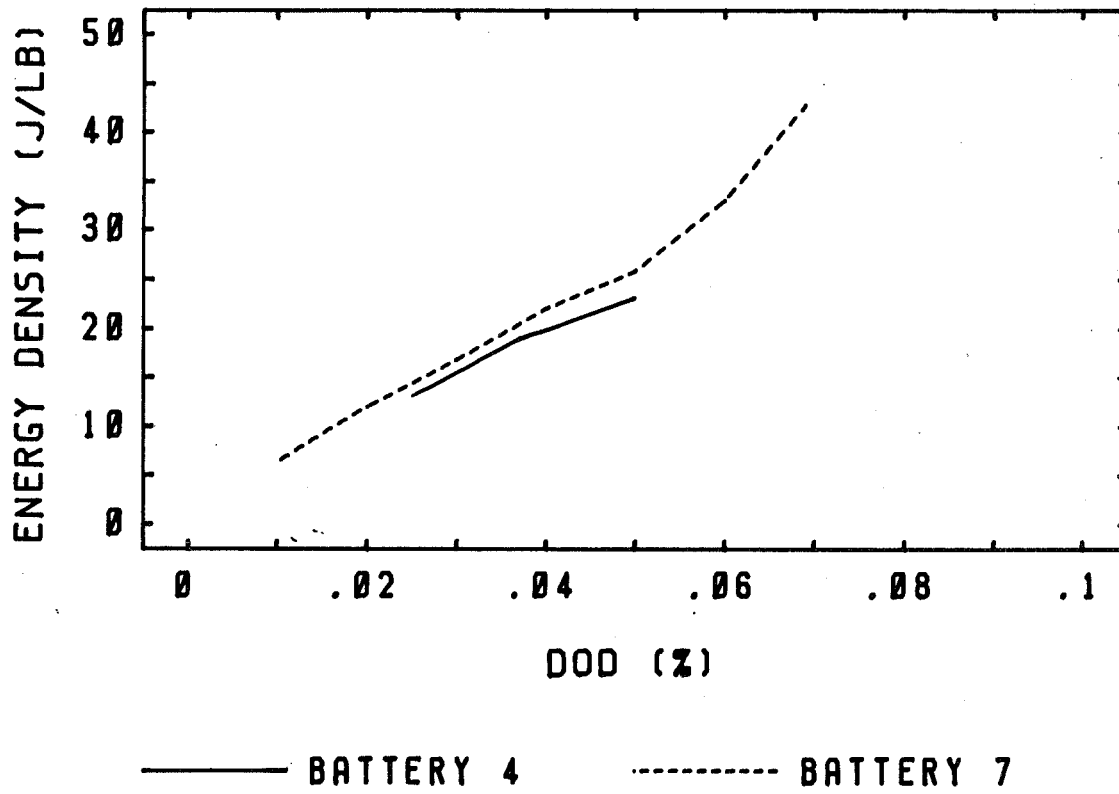
Figure 7. Energy Density Versus DOD
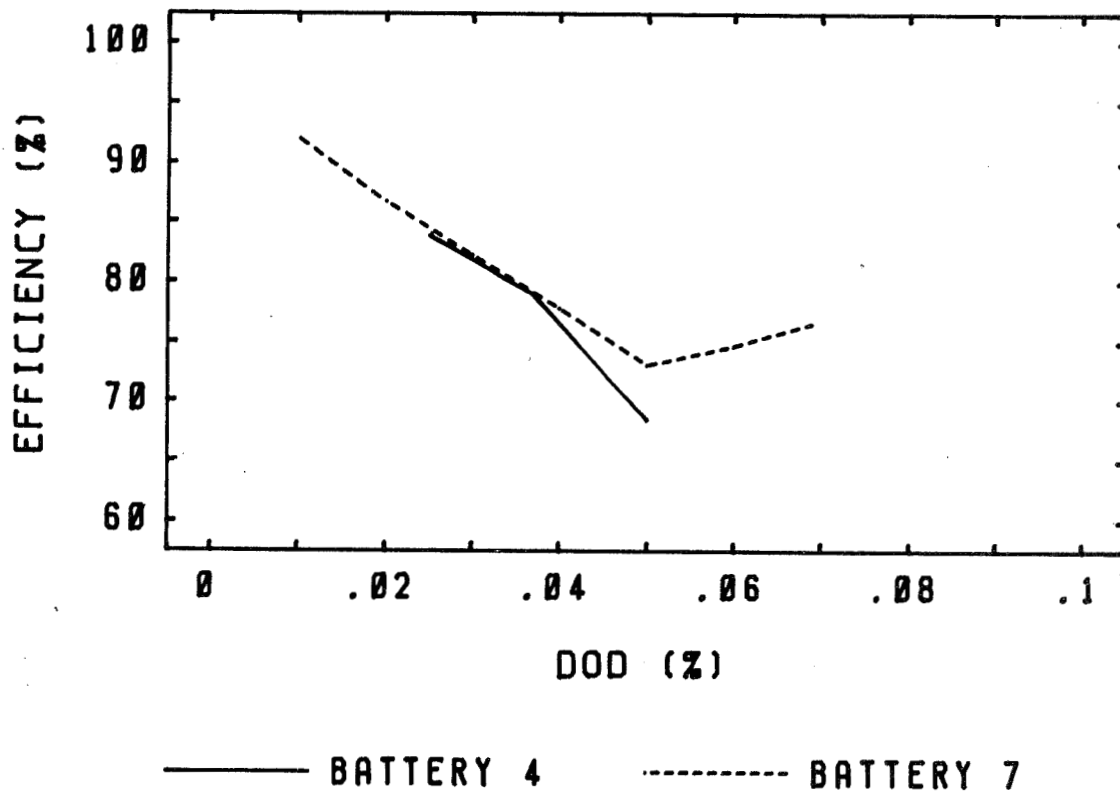
Figure 8. Efficiency Versus DOD
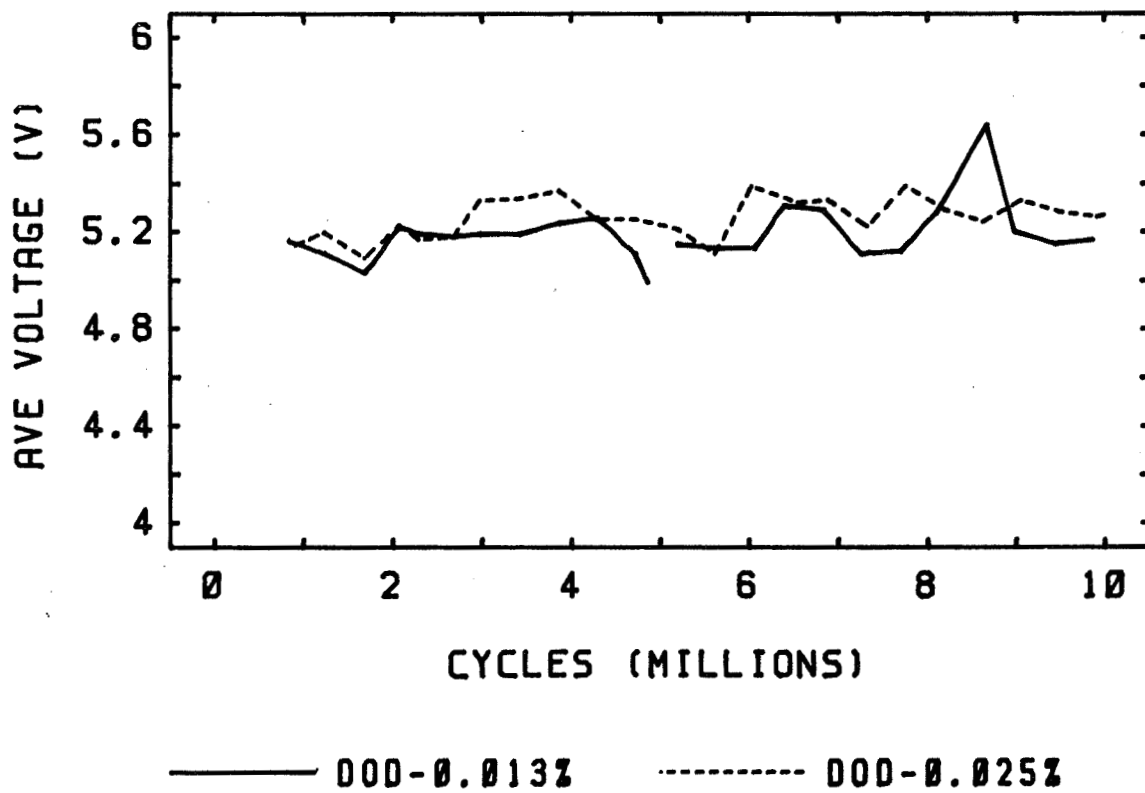
Figure 9. Average Battery Voltage Versus Cycles
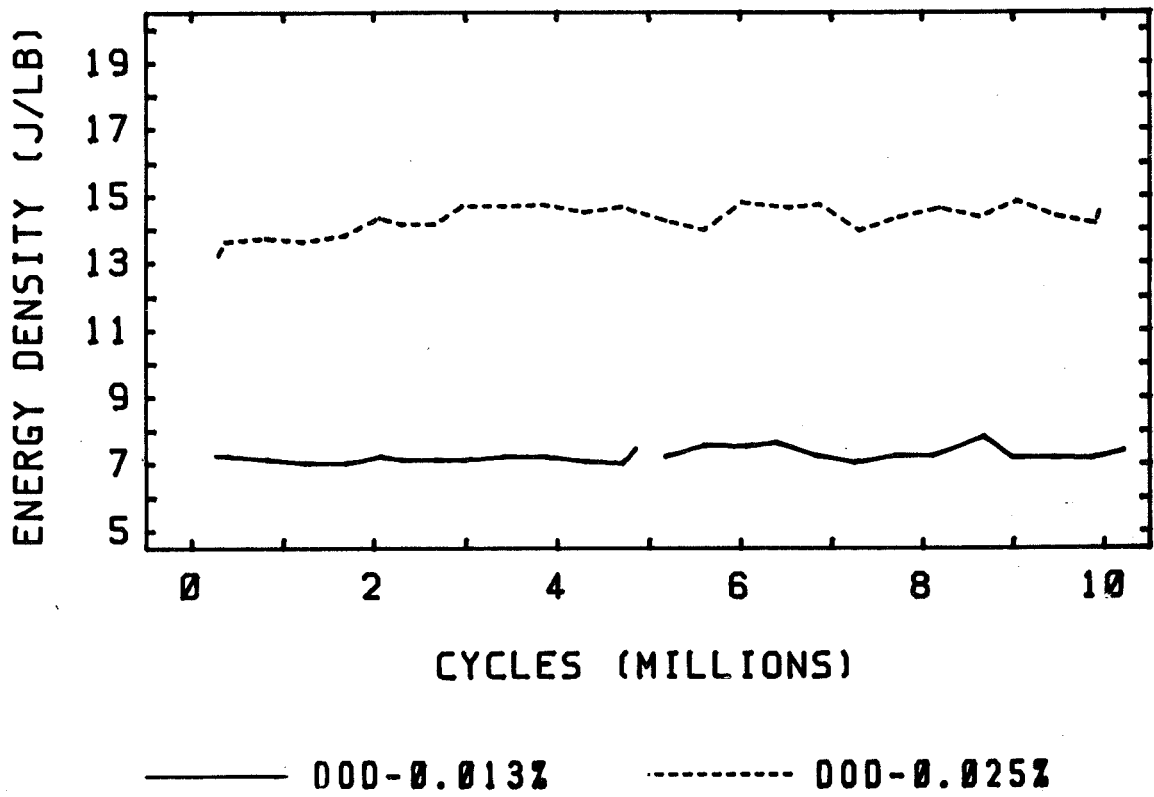
Figure 10. Energy Density Versus Cycles
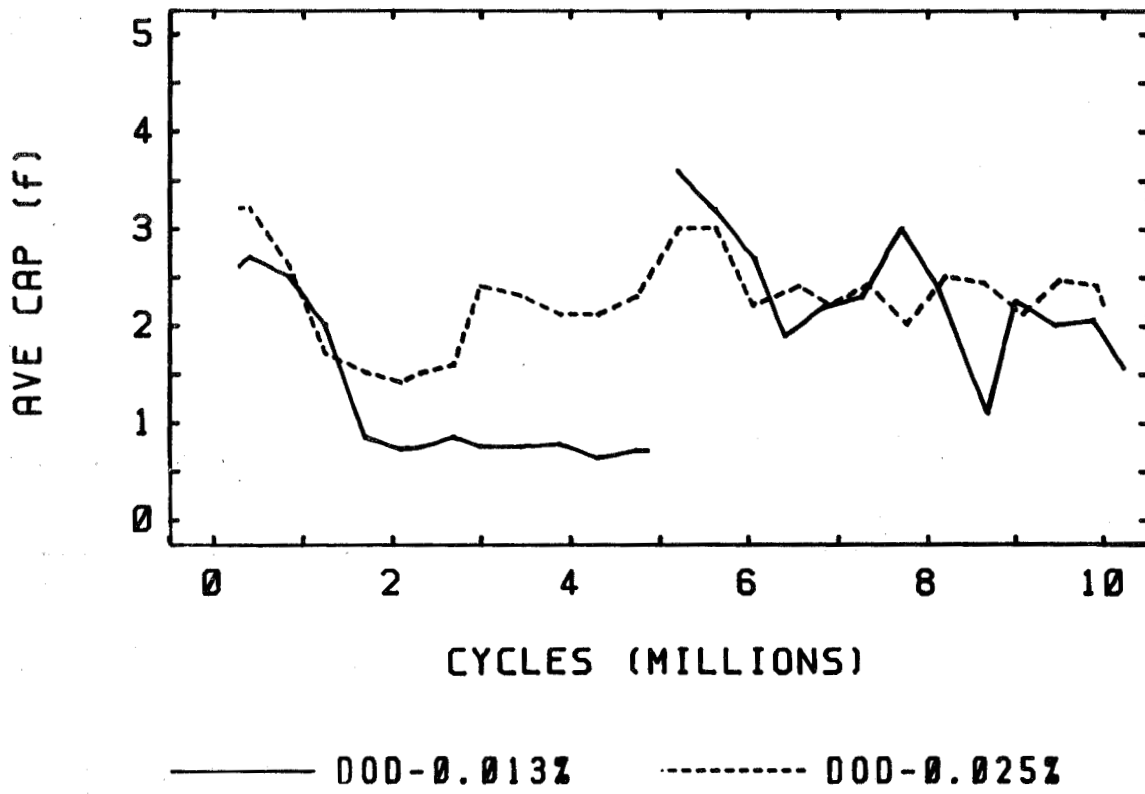
Figure 11. Average Capacitance Versus Cycles
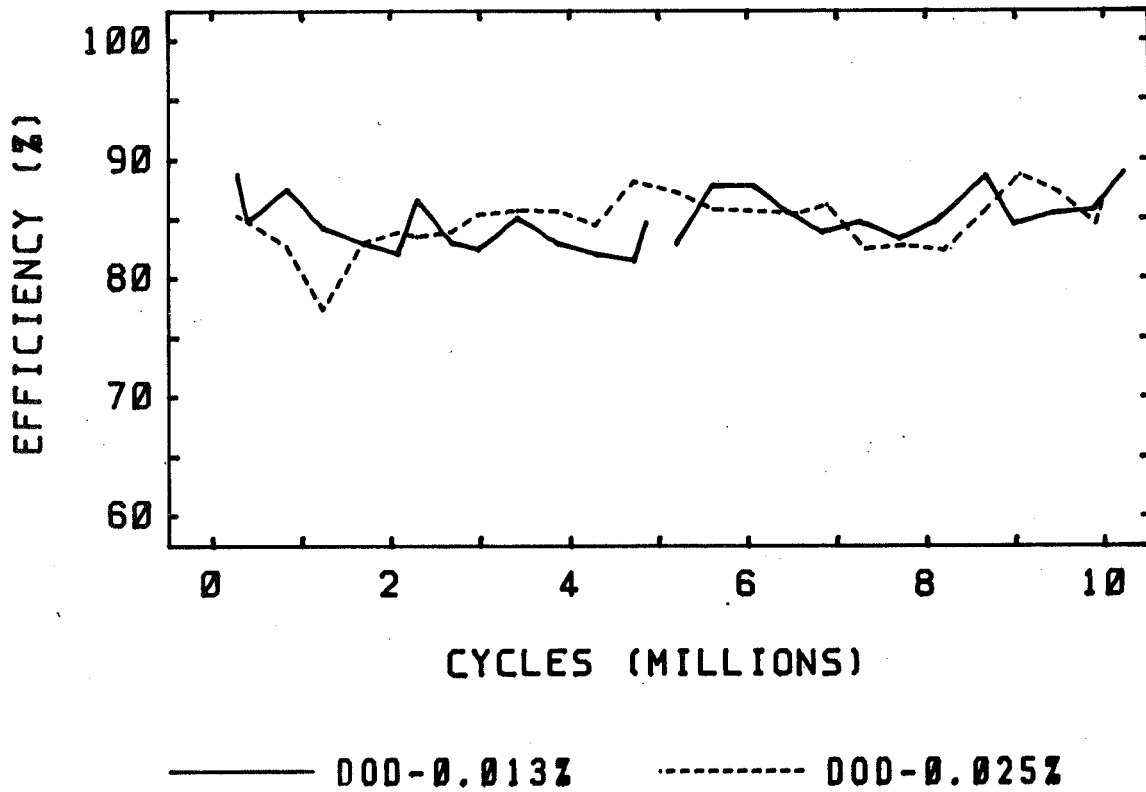
Figure 12. Efficiency Versus Cycles
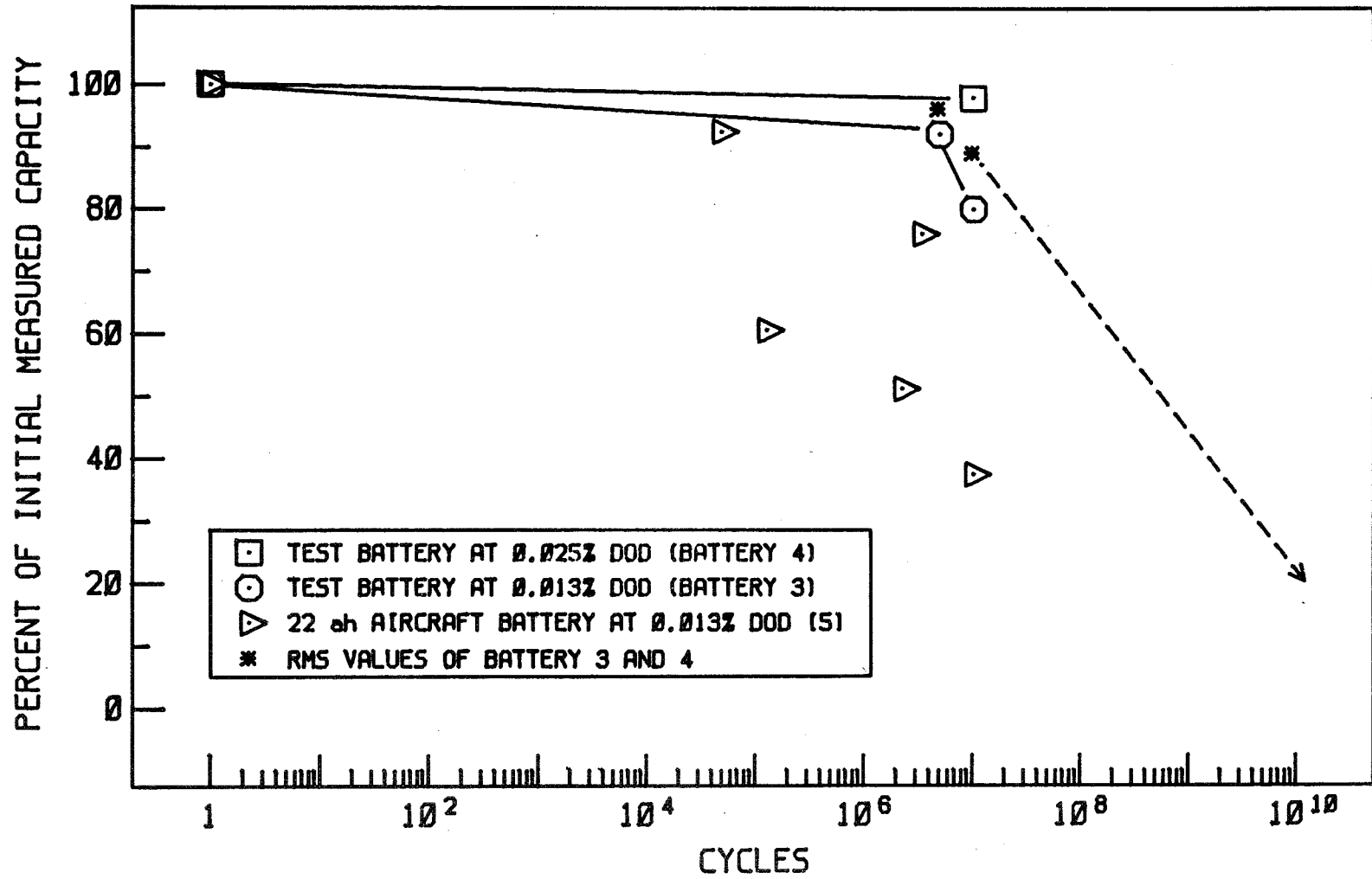
Figure 13. Percent Capacity Remaining Versus Cycles

313
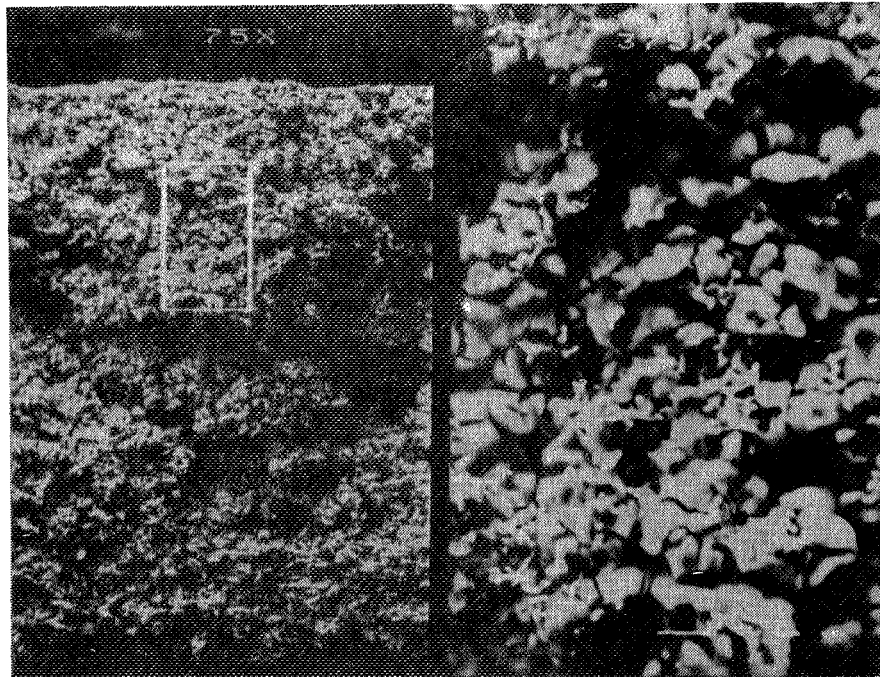
Figure 14. Uncycled Nickel Electrode (75X, 375X
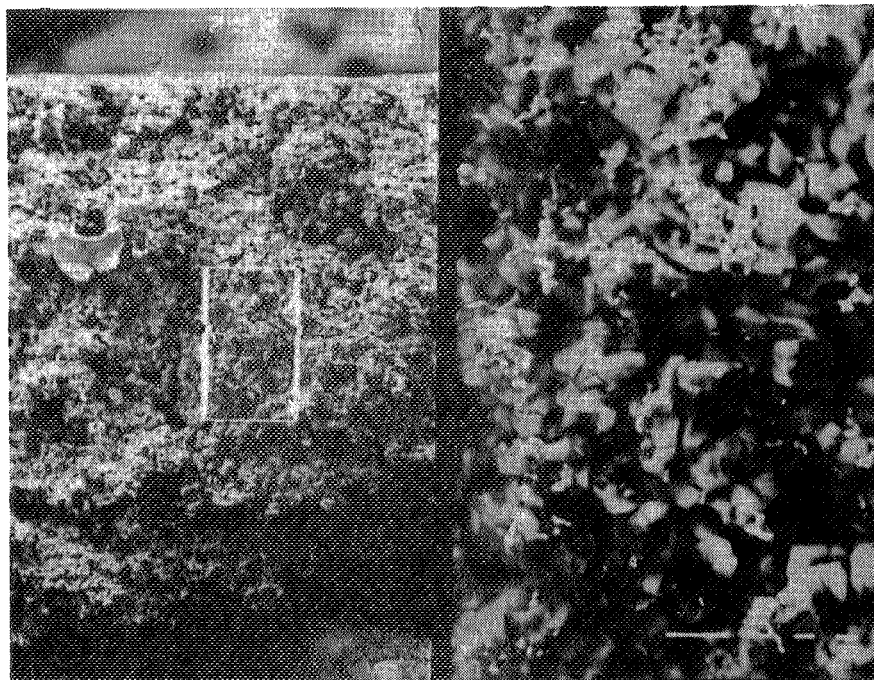
Figure 15. Cycled Nickel Electrode (75X, 375X)
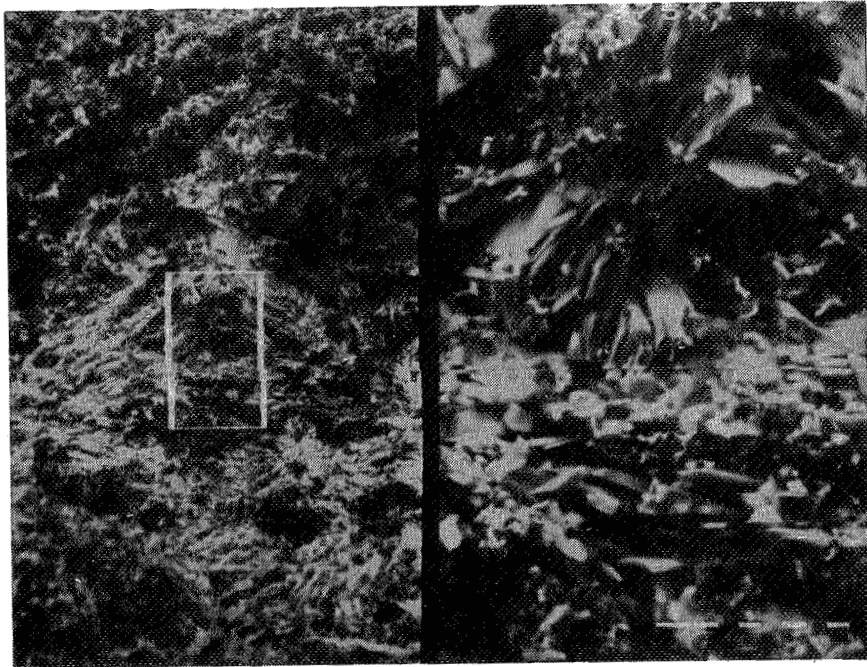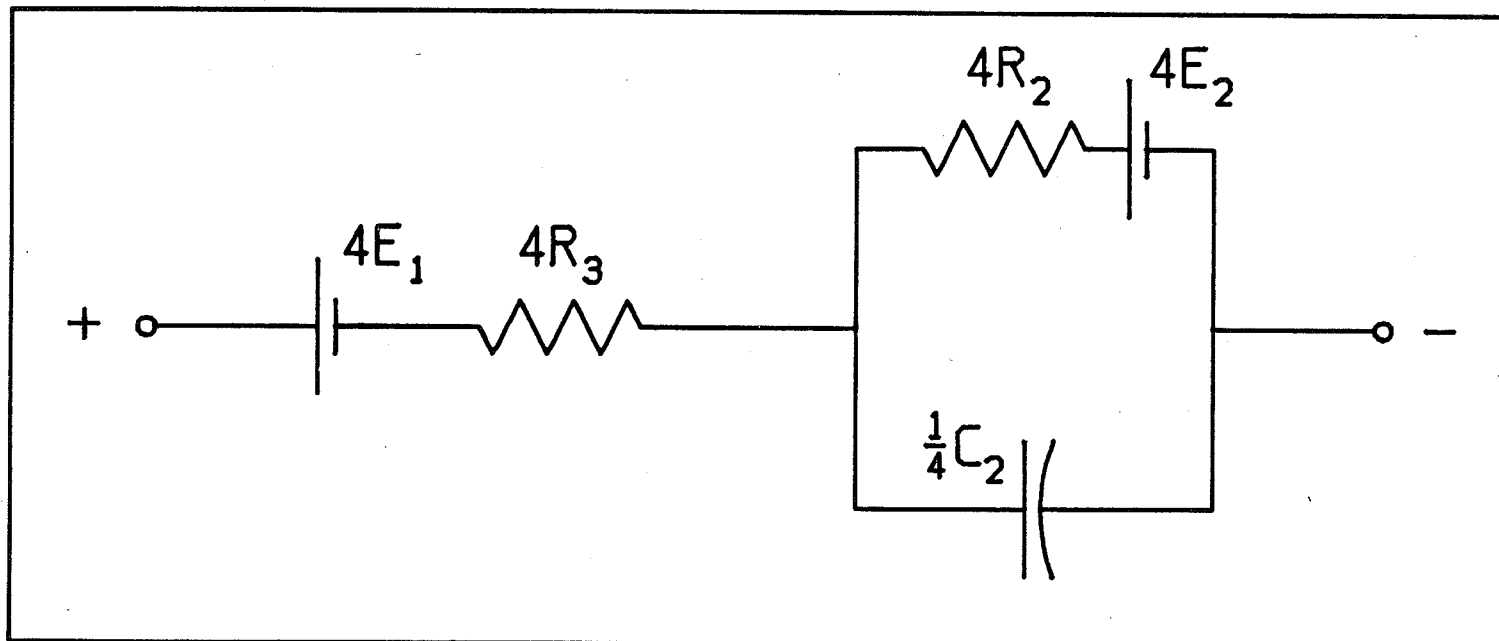
Figure 16. Uncycled Cadmium Electrode (75X, 375X)
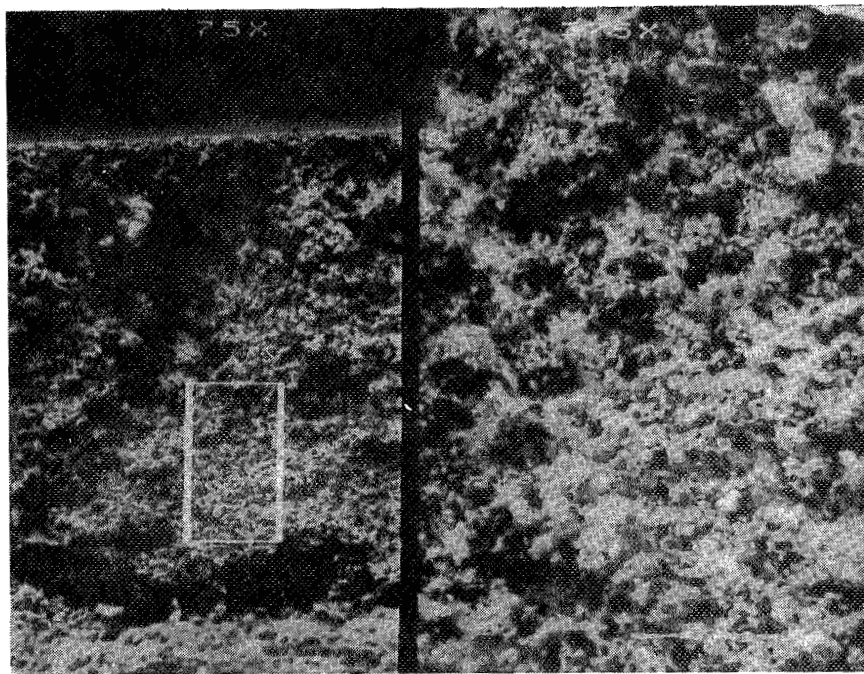
Figure 17. Cycled Cadmium Electrode (75X, 375X)
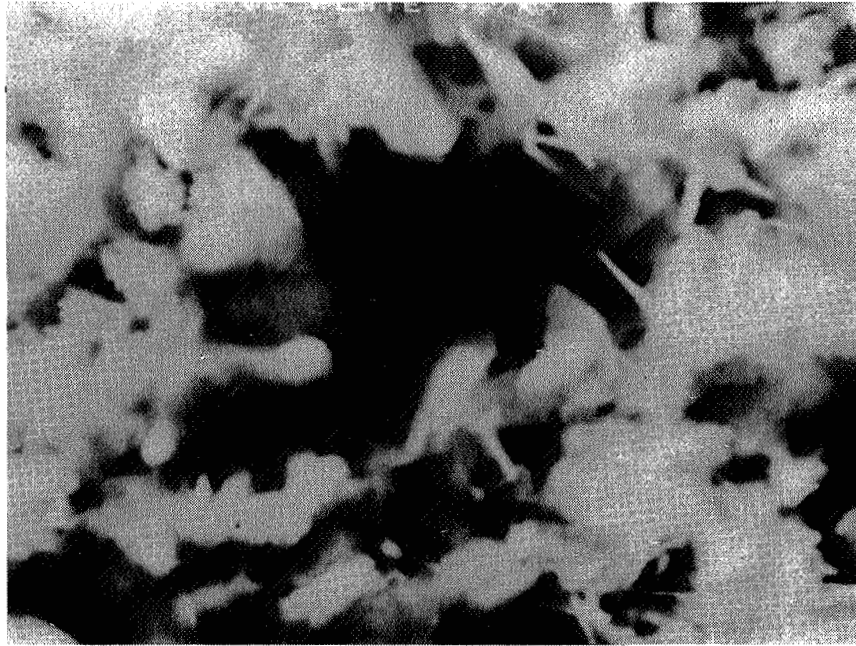
Figure 18. Uncycled Cadmium Electrode (3700X)

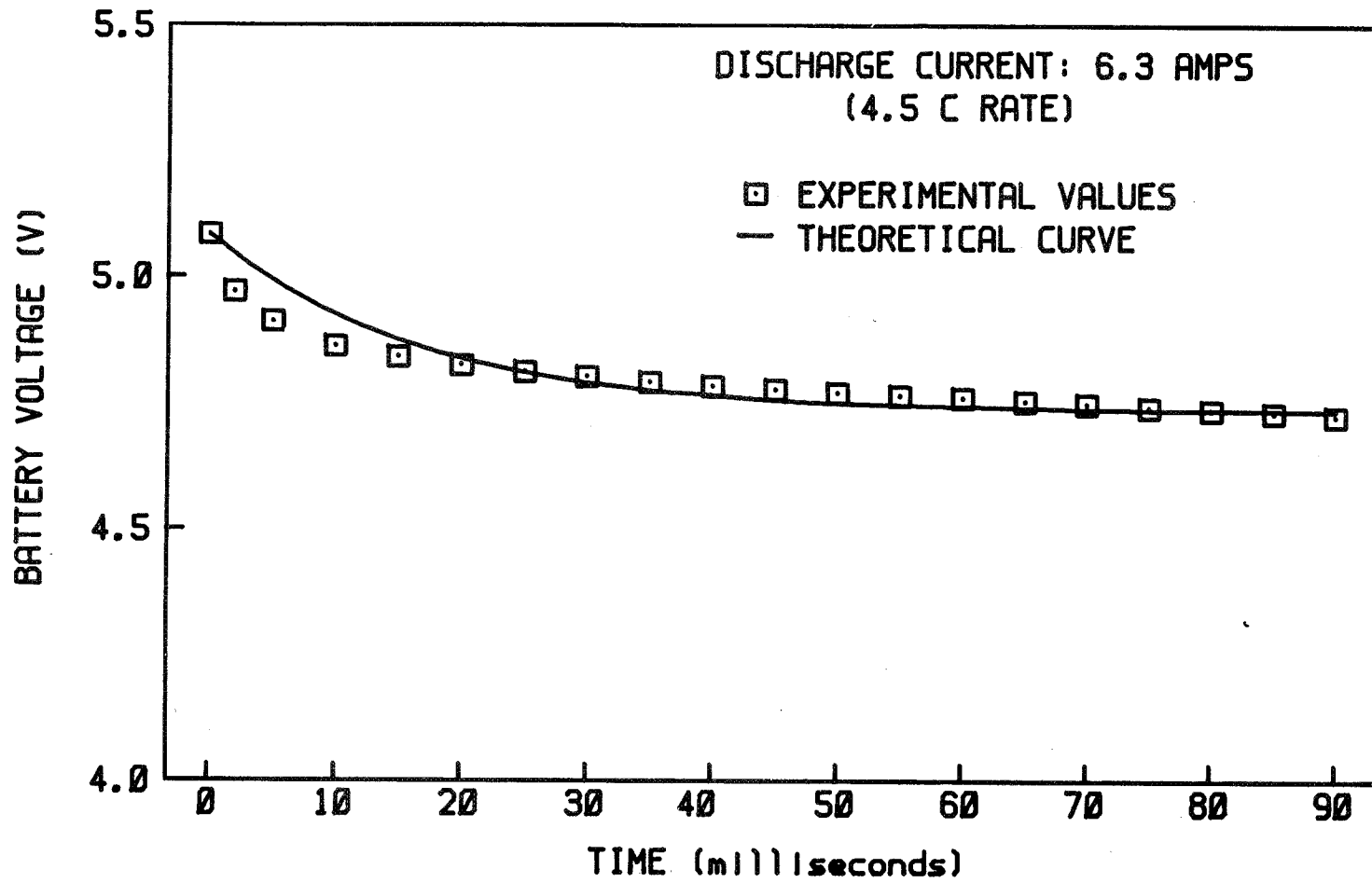Figure 19. Simplified Nickel Cadmium Battery Equivalent Circuit

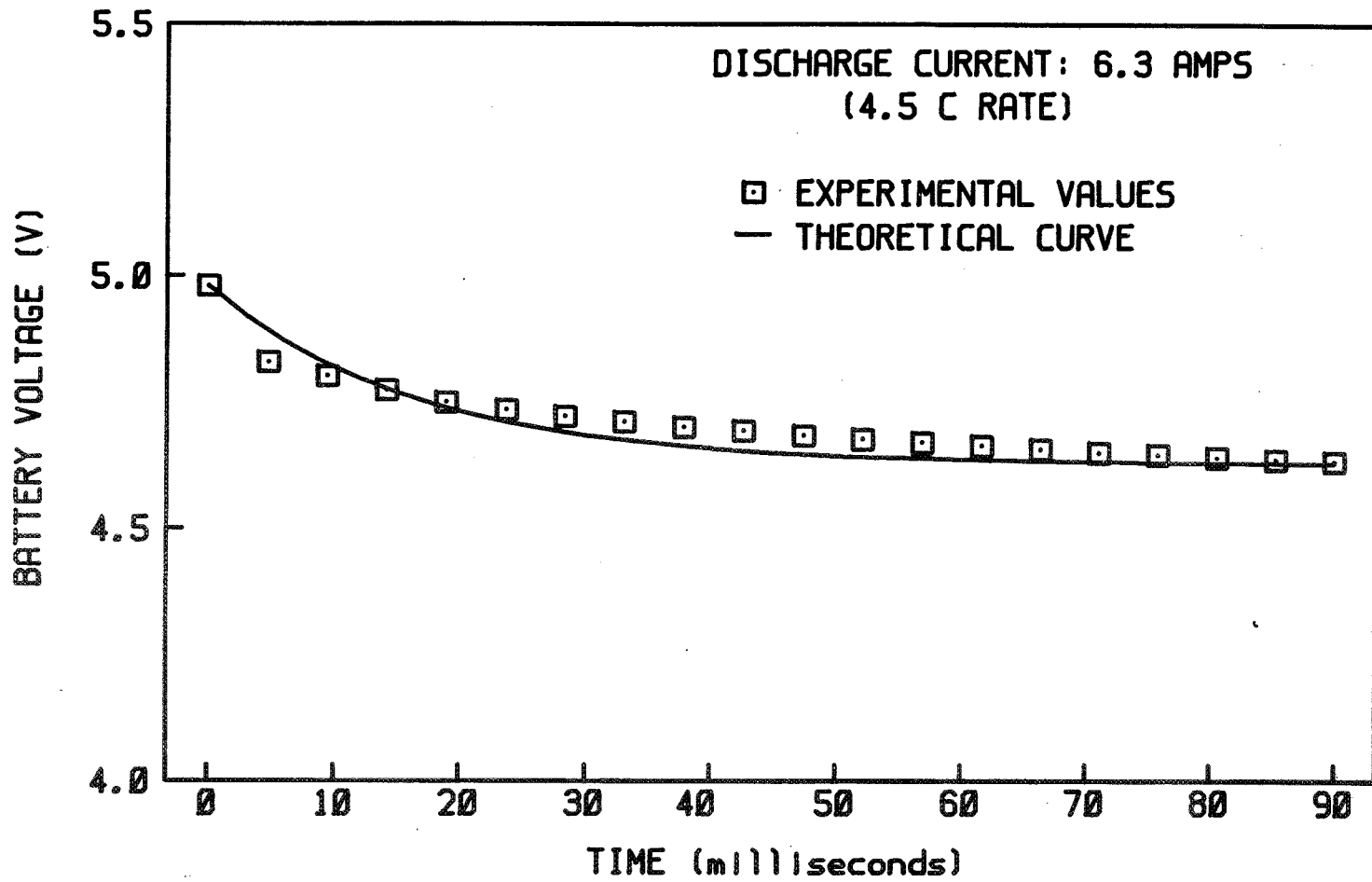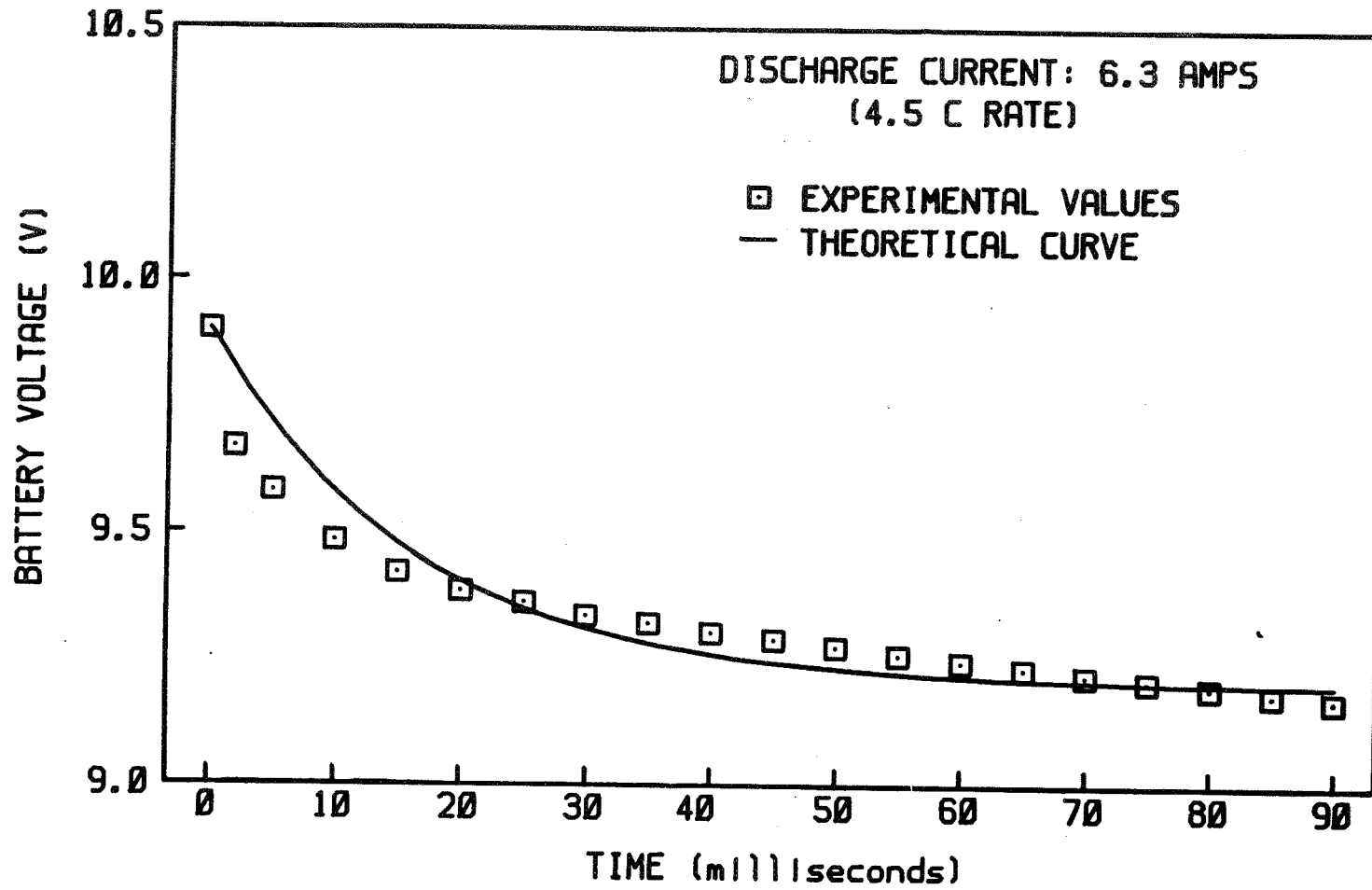Figure 20. Battery 3 Discharge Voltage

Figure 21. Battery 4 Discharge Voltage

Figure 22. Battery 3 + 4 Discharge Voltage